

UNBALANCED LATTICE SWITCHED-CURRENT FILTERS

Antônio Carlos M. de Queiroz

COPPE/EE - Electrical Engineering Program
Federal University of Rio de Janeiro
CP 68504, 21945-970 Rio de Janeiro, RJ, Brazil

ABSTRACT

This paper shows how switched-current filters can be derived from passive filters obtained by the unbalancing of doubly terminated LC lattice structures. The process is similar to what would be done for the simulation of more conventional ladder structures, but the use of lattice prototypes allows the realization in an almost physically symmetrical structure. A comparison of sensitivity characteristics between second-generation and component-simulation switched-current filters is also shown.

I. INTRODUCTION

Unbalanced lattice structures are an alternative form for the construction of passive LC doubly terminated filters [1]. For the low-pass case, these structures can be interpreted as a different form of creating transmission zeros in a basic ladder realizing a polynomial filter. Instead of creating zeros locally by adding reactive elements that form series of parallel LC tanks with the elements of the basic polynomial ladder, the elements are added coupling elements at opposite sides of the ladder, always keeping the symmetry of the structure. The passive structures can assume several different forms [1][2][3], all convertible one to the other by simple circuit transformations. For odd-order low-pass filters (only low-pass filters will be discussed in this work), the network between the terminations is composed of a series of π and T networks, one inside the other, that can also be drawn as a three-sided pyramid or ladder. For even-order approximations, complex symmetrical networks presenting imaginary resistors result, that have real equivalents formed by two identical ladders coupled by gyrators.

These structures share with the conventional LC doubly terminated ladder structures the properties of low passband sensitivity due to maximum power transfer, being frequently even better than conventional ladder structures in this aspect. They can also provide solutions for the realization of approximations where the conventional ladder realization is not possible, as for filters with small passband ripple and low stopband attenuation, particularly filters using the inverse Chebyshev approximation. The structures are always symmetrical, a property that can simplify the layout of integrated filters simulating the passive structures, turns them more insensitive to gradients in process parameters or temperature, and the symmetry by itself guarantees, in most cases, that the filter presents low sensitivity to variations on its components [1][2].

As weak points, unbalanced lattice structures present relatively high stopband sensitivities, due to the large number of elements involved in the formation of the transmission zeros, and may present larger dispersion in element values, when compared with conventional

ladder structures. For low-order filters, up to orders 5 or 6, however, these problems are not so significant.

A synthesis procedure for these filters was developed in [2] and already described in [1][3]. Certainly, more conventional procedures for the design of lattice structures and their unbalancing can also be used. A computer program that can generate unbalanced lattice structures, and also conventional ladders, can be found in [4].

II. UNBALANCED LATTICE FILTERS

Two example filters will be used in this paper. A 5th-order elliptic filter and a 4th-order modified elliptic filter, with a transmission zero moved to infinity to allow an LC doubly terminated realization. Both filters were obtained using [4]. The normalized prototype structures are shown in Figs. 1 and 2.

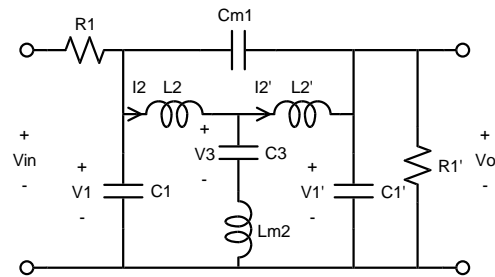


Fig. 1. Unbalanced lattice 5th-order elliptic filter. $R_1=1\Omega$, $C_1=1.9928\text{ F}$, $C_{m1}=0.1068\text{ F}$, $C_3=1.2259\text{ F}$, $L_2=0.7096\text{ H}$, $L_{m2}=0.6064\text{ H}$.

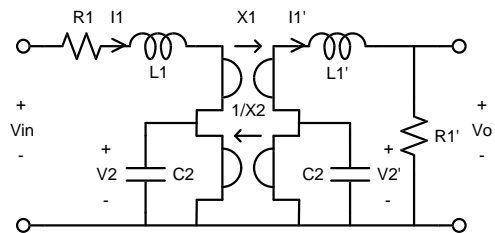


Fig. 2. Unbalanced lattice 4th-order modified elliptic filter. $R_1=1\Omega$, $L_1=2.0514\text{ H}$, $C_2=1.0713\text{ F}$, $X_1=0.2226\Omega$, $X_2=1.4083\text{ 1}/\Omega$.

The filters were predistorted for passband border at 1/10 of the sampling frequency, using the bilinear transformation. With the period of the normalized sampling frequency being $T=2\pi/10=0.6283$ seconds, the passband border of the normalized switched filters is at 1 Hz for a switching frequency of 10 Hz if the passband border of the prototypes is at 1.034 rad/s, what corresponds to the values listed. Both filters were designed with maximum passband attenuation of 1 dB and minimum stopband attenuation of 40 dB.

Note that with these specifications, both filters are also realizable by conventional ladder structures.

III. “SECOND GENERATION” SI REALIZATIONS

Unbalanced lattice structures can be easily simulated in SI implementation with the use of true bilinear integrators. A simple bilinear integrator using a “second generation” structure is shown in Fig. 3. It’s based on single transistor memory cells, what reduces the sensitivity to mismatches of the structure, and is operated by two clock signals without overlap (1, 2), but for safe operation requires two other special clock signals (1’, 2’), and a point x to where redirect the input current in phase 2, as described in [5]. It seems to be also possible to obtain exact realizations based on Euler integrators [5], but the structure or the unbalanced lattice is not adequate for simple transformations leading to those realizations, that are somewhat more sensitive to mismatches, anyway.

Note that an actual implementation would have to include some extra transistors, as cascodes, regulated cascodes, or equivalent structures, to increase the ratio between output and input impedances of the SI cells. The basic structures will be used in this work only for simplicity, as only the methods for the generation of the basic structures are discussed.

The transfer function in z transform for the circuit in Fig. 3, assuming input and output at phase 1, is easily obtained as eq. (1).

$$T_{11}(z) = \frac{I_{BI,1}}{I_{i,1}} = K \frac{1 + z^{-1}}{1 - z^{-1}} \quad (1)$$

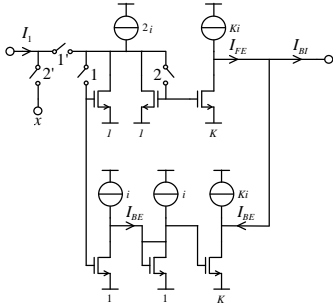


Fig. 3. Basic structure for a true bilinear 2nd-generation SI integrator.

Considering the 5th-order structure in Fig. 1, a set of modified state equations in integral form (including instantaneous couplings due to the capacitor loops and inductor cut-sets that form the transmission zeros) can be obtained as eqs. (2). Replacing the bilinear equivalence, eq. (3), in eqs. (2), a series of bilinear integrators are obtained, that correspond to the possible SI realization shown in Fig. 4. Note how the direct couplings are implemented, by using input circuits that cancel the poles of the integrators with zeros, and how the inverters can be grouped at the output of the integrators. The direct couplings between V_1 and V_1' require extra inverters. The element values are obtained as eqs. (4). The values listed are widths of the transistors, relative to the “unitary” transistors shown marked with “1” in Fig. 4, assuming that their lengths are identical. It’s also

assumed that all transistors are biased with currents proportional to their widths, not shown in the schematic drawing. A scaling factor for the input current is also listed. Due to the symmetry of the prototype, not many different widths are required in the transistors, if dynamic range scaling is not performed in the structure. With these values the internal signal current levels follow what happens with voltages and currents in the passive prototype.

$$\begin{aligned} V_1 &= \frac{\left(\frac{V_{in}}{R_1} - I_2 - \frac{V_1}{R_1} \right)}{s(C_1 + C_{m1})} + \frac{C_{m1} V_1'}{C_1 + C_{m1}} \\ I_2 &= \frac{1}{s(L_2 + L_{m2})} (V_1 - V_3) + \frac{L_{m2} I_2'}{(L_2 + L_{m2})} \\ V_3 &= \frac{I_2 - I_2'}{sC_3} \end{aligned} \quad (2)$$

$$\begin{aligned} I_2' &= \frac{1}{s(L_2' + L_{m2})} (V_3 - V_1') + \frac{L_{m2} I_2}{(L_2' + L_{m2})} \\ V_1' &= \frac{\left(I_2' - \frac{V_1'}{R_1'} \right)}{s(C_1' + C_{m1})} + \frac{C_{m1} V_1}{C_1' + C_{m1}} \end{aligned} \quad (3)$$

$$\frac{1}{s} = \frac{T}{2} \frac{1 + z^{-1}}{1 - z^{-1}} \quad (3)$$

Following a similar procedure, the even-order structure in Fig. 2 can also be simulated. The resulting structure is also basically symmetrical and similar to the odd-order case, with the only differences being that there are no direct couplings between the integrators and that the couplings through the gyrators in Fig. 2 appear as normal extra bilinear inputs in the integrators, causing a break in the symmetry due to the extra inverters required. The resulting structure is shown in Fig. 5, with the element values listed as eqs. (5). Two extra inverters appear again in the implementation of the gyrators.

These realizations are quite good in terms of sensitivity characteristics, because the bilinear transformation maps all the sensitivities of the passive prototype into the values of the elements in the SI structure, with the exception of the elements realizing the direct couplings, that appear quadruplicated. The denominators of the integral operators are naturally correct due to the use of single transistor memory cells. The current subtractors have no correspondent in the passive structure, but the effect of mismatches in them is small at the passband of the filter, because they are responsible only for the generation of the averaging of successive input samples at the numerator of each bilinear integration, or the creation of a transmission zero at $z=-1$ at each integration. They affect more strongly the behavior of the filter around $\frac{1}{2}$ of the switching frequency, far into the stopband.

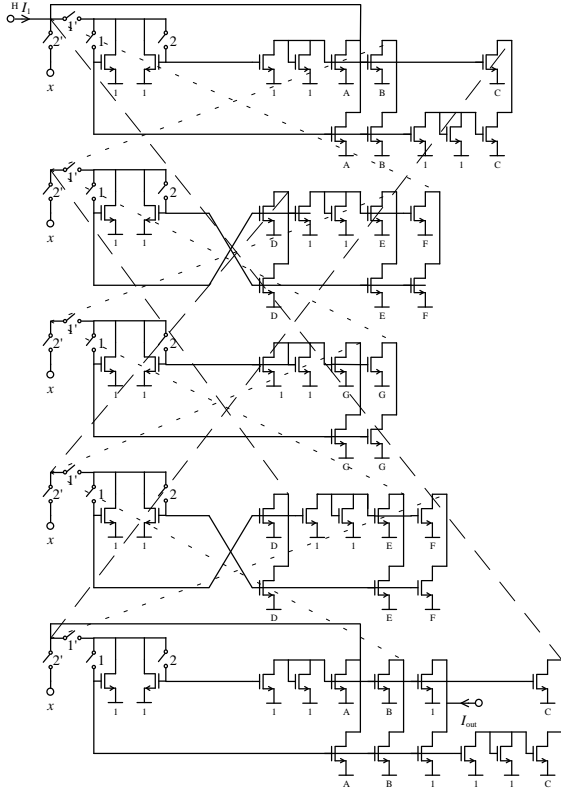


Fig. 4. Schematic normalized second generation SI implementation for the 5th-order filter in Fig. 1.

$$\begin{aligned}
 A &= T/R_1/(C_1 + C_{m1})/2 & E &= T/C_3/2 \\
 B &= T/(L_2 + L_{m2})/2 & F &= T/(C_1 + C_{m1})/2 \\
 C &= C_{m1}/(C_1 + C_{m1}) & G &= T/(L_2 + L_{m2})/2 \\
 D &= L_{m2}/(L_2 + L_{m2}) & H &= T/R_1/(C_1 + C_{m1})/2
 \end{aligned} \quad (4)$$

Equivalent structures derived from conventional ladder structures would require less current inverters (just five and four, for the two filters shown), would have somewhat smaller stopband sensitivities, but at most similar passband sensitivities.

IV. “COMPONENT-SIMULATION” SI REALIZATIONS

This technique is described in [6] for conventional ladder filters. Here it will be applied in the form described in [7], using modulated signals, bilinear integrations, and swapping of components with opposite sensitivities, to obtain filters that have better sensitivity characteristics. These filters are obtained by departing from continuous-time versions of the passive prototypes made from transconductors and transcapacitors, and then by the substitution of these components, one by one, by equivalent SI structures. It's easy then to group all the inverters at the input of “node” blocks, and the resulting structures have always a fixed number of inverters. The phase-to-phase symmetry in the operation of the filters make them work with an effective sampling frequency that is twice the switching frequency. They operate safely with just two

nonoverlapping clock signals, because there is no switch that conducts current all the time. The symmetry allows the swapping phase to phase of elements that have opposite sensitivities, what effectively eliminates mismatch errors caused by them [7]. For the filters in Figs. 1 and 2, the corresponding realizations are shown in Figs. 6 and 7, also with bias sources omitted. The realizations shown swap the elements of the “voltage inverters” at the input of the “nodes”, and some other elements that account for most of the functionality of the terminations and gyrators that couple capacitive and inductive elements. Fig. 8 shows the passband of the 5th-order filter, with error limits computed by sensitivity analysis [8] shown, where it can be seen that it's less sensitive. The 4th-order filter (not shown) results in some advantage to the 2nd-generation structure, because of the several unswapped elements, corresponding to the gyrators, that remain in the structure in Fig. 7, and of the absence of direct couplings between the integrators in the structure in Fig. 3, what results in better preservation of the sensitivity characteristics of the passive prototype. For this reason, even-order unbalanced lattice filters are particularly convenient for realizations based on integrators.

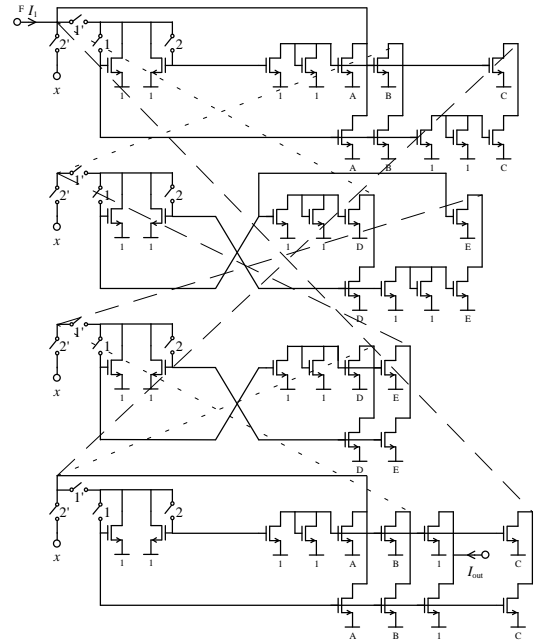


Fig. 5. Schematic normalized second generation SI implementation for the 4th-order filter in Fig. 2.

$$\begin{aligned}
 A &= TR_1/L_1/2 & D &= T/L_1/2 \\
 B &= T/C_2/2 & E &= T/X_2/C_2/2 \\
 C &= TX_1/L_1/2 & F &= TR_1/L_1/2
 \end{aligned} \quad (5)$$

V. CONCLUSIONS

Two different techniques for the generation of SI filters from unbalanced lattice passive prototypes were presented. They present low sensitivity characteristics, and are as systematically designable as their equivalents obtained from conventional ladder structures. As advantages they present better symmetry of structure, with less different element values, and the unbalanced lattice can provide

solutions to filters that can't be realized by ladder structures. This work also shows more complex examples of the component-simulation SI technique, using the minimum sensitivity technique developed in [7].

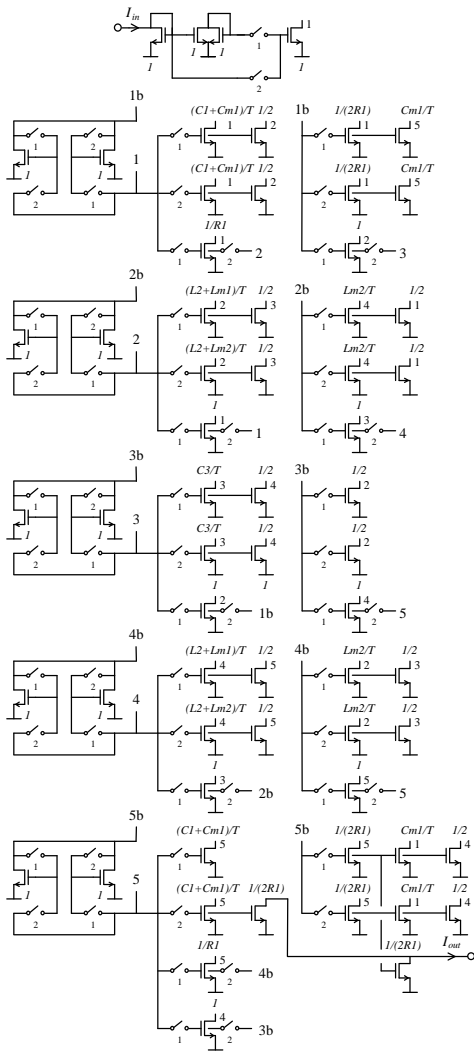


Fig. 6 Schematic component-simulation SI realization for the 5th-order filter in Fig. 1.

REFERENCES

- [1] A. C. M. de Queiroz and L. P. Calôba, "Passive symmetrical RLC filters suitable for active simulation", Proc. IEEE ISCAS, Espoo, Finland, May 1988, pp. 2411-2414.
- [2] A. C. M. de Queiroz, "Filtros Analógicos com Simetria ou Antimetria Física", D. Sc. Thesis, COPPE, Federal University of Rio de Janeiro, December 1990.
- [3] A. C. M. de Queiroz and L. P. Calôba, "OTA-C filters derived from unbalanced lattice passive structures", 1993 IEEE ISCAS, Chicago, USA, May 1993, pp. 2256-2259.
- [4] A. C. M. de Queiroz, Eletsim program, available at <ftp://coe.ufrj.br/pub/acmq>.
- [5] A. C. M. de Queiroz and P. R. M. Pinheiro, "Bilinear switched-current ladder filters using Euler integrators". IEEE Trans. Circuits and Systems-II, vol. 43, no. 1, January 1996, pp. 66-70.

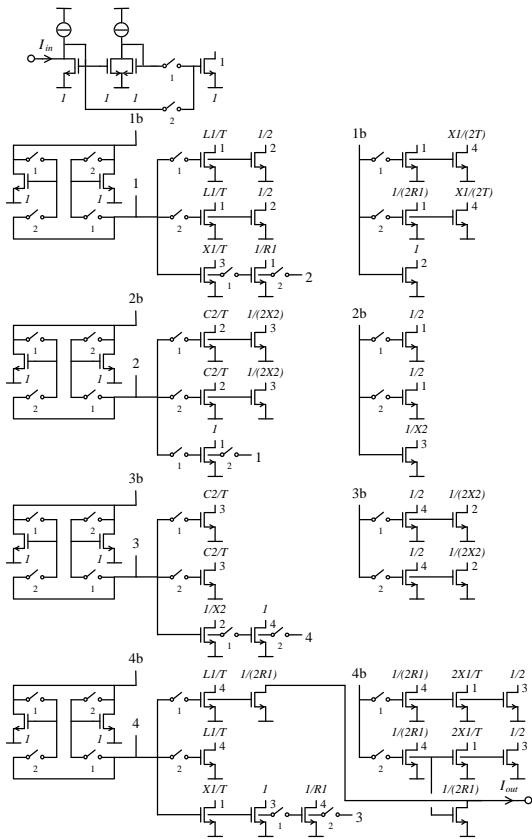


Fig. 7. Schematic component-simulation SI realization for the 4th-order filter in Fig. 2.

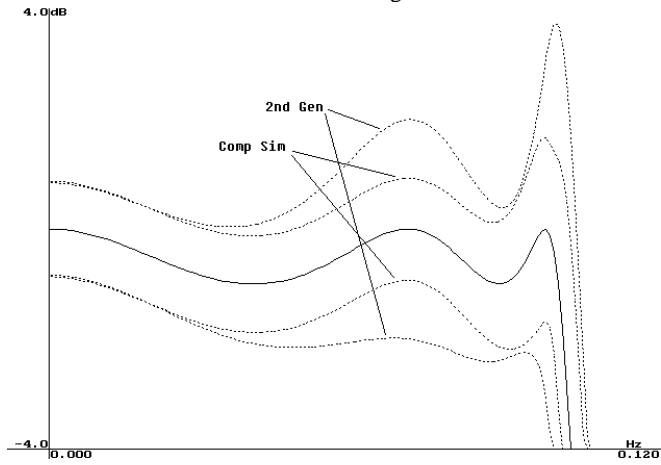


Fig. 8. Passband gain curve with error margins for the filters in Figs. 4 and 6, assuming 5% of error in all the element values.

- [6] J. Schechtman, A. C. M. de Queiroz, and L. P. Calôba, "Switched-current filters by component simulation", Analog Int. Circ. and Signal Proc., vol. 13, no. 3, July 1997, pp. 303-309.
- [7] A. C. M. de Queiroz and J. Schechtman, "Sensitivity and error reduction by component swapping in switched-current filters", 1999 IEEE ISCAS, Orlando, USA, May 1999, pp. 480-483.
- [8] A. C. M. de Queiroz, P. R. M. Pinheiro, and L. P. Calôba, "Nodal analysis of switched-current filters". IEEE Trans. Circuits and Systems-II, vol. 40, no. 1, January 1993, pp. 10-18.